SE 276C/MAE 232C: Nolinear and Advanced Finite Elements Method

Final Project Report, Option 2

Name: Ru Xiang

Date: June 12th, 2019

1 Problem Statement

In this problem, we have a cantilever beam of length $L = 50in$, height $D = 10in$, subjected to a shear load $P = 250lb$ at the end. The beam is made of a hyperelastic material described by Saint Venant-Kirchhoff model.

$$W = \frac{1}{2} C^s_{ijkl} E_{ij} E_{kl}$$

where

$$C^s_{ijkl} = \lambda \delta_{ij} \delta_{kl} + \mu(\delta_{ik}\delta_{jl} + \delta_{il}\delta_{jk})$$

$$\lambda = \frac{\nu E}{(1+\nu)(1-2\nu)}$$

$$\mu = \frac{E}{2(1+\nu)}$$

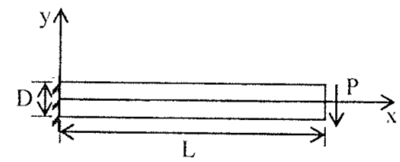

Figure 1. Beam subjected to a tip shear load

Figure 1: 2D plane-strain cantilever beam problem.

To solve this problem, we used the following finite element formulations:

- 2D plane-strain model, 4-node quadrilateral (Q4) elements.
- Saint Venant-Kirchhoff strain engergy density function.
- Total Lagrangian Formulation.
- Three integration methods: Full Integration **(FI)**, Reduced Integration **(RI)** and Selective Reduced Integration **(SRI)**.

2 Numerical Formulation and Computational Procedures

MAE 232C Final Project Ru Xiang.

$\boxed{\text{Formulation}}$ Given D, L, P (load)

material: E, ν

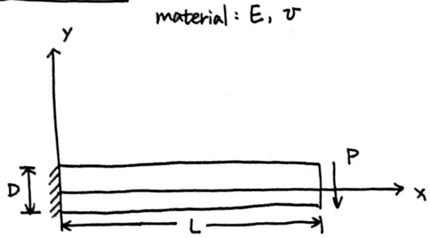

Saint Venant-Kirchhoff Model:

$$W = \frac{1}{2} C^s_{ijkl} E_{ij} E_{kl}$$

where $C^s_{ijkl} = \underbrace{\lambda \delta_{ij} \delta_{kl}}_{C^s_\lambda} + \underbrace{\mu (\delta_{ik}\delta_{jl} + \delta_{il}\delta_{jk})}_{C^s_\mu}$

$$\lambda = \frac{\nu E}{(1+\nu)(1-2\nu)}$$

$$\mu = \frac{E}{2(1+\nu)}$$

1. Equilibrium equation:

$\underset{\sim}{x}^\nu = \underset{\sim}{X} + \underset{\sim}{u}^\nu(\underset{\sim}{X}, t)$ iteration ν

$\underset{\sim}{x}^{\nu+1} = \underset{\sim}{X} + \underset{\sim}{u}^{\nu+1}(\underset{\sim}{X}, t)$ iteration $\nu+1$

$\tau^\nu_{ij,j} + b_i = 0$ in Ω_{x^ν}

$\tau^\nu_{ij} n_j = h_i$ in $\Gamma^{h_i}_{x^\nu}$ (natural BC) $= \underset{\sim}{X} + \underset{\sim}{u}^\nu(\underset{\sim}{X}, t) + \Delta \underset{\sim}{u}(\underset{\sim}{X}, t)$

$u_i = g_i$ on $\Gamma^{g_i}_{x^\nu}$ (essential BC) $= \underset{\sim}{x}^\nu + \Delta \underset{\sim}{u}(\underset{\sim}{X}, t)$

2. Variational Equation of Equilibrium:

Given $\underset{\sim}{u}(\underset{\sim}{x}^\nu, t) \rightarrow \underset{\sim}{\tau}^\nu$. Find $\underset{\sim}{u}(\underset{\sim}{x}^{\nu+1}, t)$ such that

Updated Lag. Formulation (in current configuration x) $\int_{\Omega_x} \delta u_{i,j} \tau_{ij}\, d\Omega - \int_{\Omega_x} \delta u_i b_i \, d\Omega - \int_{\Gamma^{h_i}_x} \delta u_i h_i \, d\Gamma = 0.$

$\updownarrow$

✓ Total Lagrangian Formulation (used in this project) (in undeformed config. X)

$$\underbrace{\int_{\Omega_X} \delta E_{ij} S_{ij} \, d\Omega}_{I_1} - \underbrace{\int_{\Omega_X} \delta u_i b^\circ_i \, d\Omega}_{I_2} - \underbrace{\int_{\Gamma^{h_i}_X} \delta u_i h^\circ_i \, d\Gamma}_{I_3} = 0.$$

3. In SVK material model: $W = \frac{1}{2} C^s_{ijkl} E_{ij} E_{kl}$

2^{nd} PK: $S_{ij} = \frac{\partial W}{\partial E_{ij}} = C^s_{ijkl} E_{kl}$ 1^{st} PK: $\sigma_{ij} = S_{ij} F_{ji}$

$$\frac{\partial S_{ij}}{\partial E_{kl}} = C^s_{ijkl}$$

Linearization:

$$E_{ij} = \frac{1}{2}(F_{ki}F_{kj} - \delta_{ij})$$

4. $I_1 = \int_{\Omega X} \delta E_{ij} S_{ij} \, d\Omega$. $\qquad \delta E_{ij} = \frac{1}{2}(\delta F_{ki} F_{kj} + F_{ki}\delta F_{kj})$

$$\Delta S_{ij} = \frac{\partial S_{ij}}{\partial E_{kl}} \Delta E_{kl}$$

$$L[I_1] = \Delta I_1 = \int_{\Omega X} [(\Delta \delta E_{ij}) S_{ij} + \delta E_{ij}(\Delta S_{ij})] \, d\Omega$$

$$= \int_{\Omega X} [\tfrac{1}{2}(\delta F_{ki} \Delta F_{kj} + \Delta F_{ki}\delta F_{kj}) S_{ij} + \delta E_{ij} C^{S}_{ijkl} \Delta E_{kl}] \, d\Omega$$

$$= \int_{\Omega X} [\delta F_{ij} \underbrace{(\delta_{ik} S_{jl})}_{T_{ijkl}:\ \text{Geometric nonlearity.}} \Delta F_{kl} + \delta F_{ij} \underbrace{(F_{ip}F_{kq} C^{S}_{pjql})}_{D_{ijkl}:\ \text{material nonlinearity}} \Delta F_{kl}] \, d\Omega$$

$$= \int_{\Omega X} \delta F_{ij} (D_{ijkl} + T_{ijkl}) \Delta F_{kl} \, d\Omega.$$

5. $I_2 = \int_{\Omega X} \delta u_i b_i^{\circ} \, d\Omega = 0$

$L[I_2] = \Delta I_2 = \int_{\Omega X} \delta u_i \Delta b_i^{\circ} \, d\Omega = 0$

in this problem. no body force. $\rightarrow I_2 = 0$.

costant load p: deformation independent.

$\rightarrow h_i = h_i^{\circ}$

$\rightarrow (I_3)^{v+1}_{n+1} = (I_3)^{v}_{n+1}$

6. $I_3 = \int_{\Omega X} \delta u_i h_i^{\circ} \, d\Omega = \int_{\Omega X} \delta \underset{\sim}{d}^T \underset{\sim}{N}^T \underset{\sim}{h}^{\circ} \, d\Omega$

$L[I_3] = \Delta I_3 = 0$

7. $(I_1)^{v+1}_{n+1} - (I_2)^{v+1}_{n+1} - (I_3)^{v+1}_{n+1} = 0$

$\Rightarrow (I_1)^{v}_{n+1} + \Delta I_1 - 0 - (I_3)^{v}_{n+1} = 0$

$\Rightarrow \Delta I_1 = (I_3)^{v}_{n+1} - (I_1)^{v}_{n+1}$

$\Rightarrow \delta \underset{\sim}{d}^T (\underset{\sim}{B}^T (\underset{\sim}{D} + \underset{\sim}{T}) \underset{\sim}{B}) \Delta \underset{\sim}{d} = \delta \underset{\sim}{d}^T \{(\underset{\sim}{f}^{ext})^{v}_{n+1} - (\underset{\sim}{f}^{int})^{v}_{n+1}\}$

$\Rightarrow$ $\underset{\sim}{K} \cdot \Delta \underset{\sim}{d} = \Delta \underset{\sim}{f}$

where $\underset{\sim}{K} = \underset{\sim}{B}^T (\underset{\sim}{D} + \underset{\sim}{T}) \underset{\sim}{B}$

$\Delta \underset{\sim}{f} = (\underset{\sim}{f}^{ext} - \underset{\sim}{f}^{int})^{v}_{n+1}$

$\underset{\sim}{f}^{ext} = \int_{\Gamma X}^{h_i} \underset{\sim}{N}^T \underset{\sim}{h}^{\circ} \, d\Omega$

$I_1 = \int_{\Omega X} \delta F_{ij} \sigma_{ji} \Rightarrow \underset{\sim}{f}^{int} = \int_{\Omega X} \underset{\sim}{B}^T \underset{\sim}{\Sigma} \, d\Omega$. $\quad$ where $\underset{\sim}{\Sigma} = \begin{bmatrix} \sigma_{11} \\ \sigma_{22} \\ \sigma_{21} \\ \sigma_{12} \end{bmatrix}$

8. $\boxed{\text{FEM}}$ $\quad u_i^h(X, t) = \sum N_I(X) \, d_{iI}(t)$

$$F_{ij} = \frac{\partial x_i}{\partial X_j} = \frac{\partial(u_i^h + X_i)}{\partial X_j} = \frac{\partial u_i^h}{\partial X_j} + \delta_{ij}$$

$$= \sum \frac{\partial N_I(X) \, d_{Ii}}{\partial X_j} + \delta_{ij}$$

$\Rightarrow \underset{\sim}{F} = \underset{\sim}{B}^T (\underset{\sim}{d})^{v+1}_{n+1} + \underset{\sim}{I}$

$$\underset{\sim}{B}_I = \begin{bmatrix} N_{I,1} & 0 \\ 0 & N_{I,2} \\ N_{I,2} & 0 \\ 0 & N_{I,1} \end{bmatrix}$$ $\leftarrow$ plane strain

$\begin{pmatrix} \text{in } X \\ 1 \rightarrow x \\ 2 \rightarrow y \end{pmatrix}$

9. Function (for computation) : $[\boldsymbol{D}, \boldsymbol{T}, \boldsymbol{\Sigma}] = SVK\_MaterialModel(\boldsymbol{F}, \boldsymbol{C}^s)$

$\Rightarrow$ $\boldsymbol{C} = \boldsymbol{F}^T \boldsymbol{F}$ (Right deformation tensor)

$\boldsymbol{E} = \frac{1}{2}(\boldsymbol{C} - \boldsymbol{1})$ (Lagrangian strain)

$\boldsymbol{D}$: $D_{ijkl} = F_{ip} F_{kq} C^s_{pjql}$

$\boldsymbol{S}$: $S_{ij} = C^s_{ijkl} E_{kl}$

$\boldsymbol{\sigma}$: $\sigma_{ij} = S_{ij} F_{ji}$

$\boldsymbol{\Sigma} = \begin{bmatrix} \sigma_{11} \\ \sigma_{22} \\ \sigma_{21} \\ \sigma_{12} \end{bmatrix}$ $\boldsymbol{T}$: $T_{ijkl} = \delta_{ik} S_{jl}$

10. MatLab Schematic design :

Step 0: Initialization : store the invariants.

D, L, P, E, ν, $\boldsymbol{C}^s$, $\boldsymbol{C}^s\_d$, $\boldsymbol{C}^s\_\nu$

B_F1 , B_R1, N-L (load steps), tol (tolerance)

Boundary Conditions , mesh ...

Step 1: Load step $n+1$

$P_{n+1} = P_n + \Delta P. \rightarrow (h_i^\circ)_{n+1}$

$\boldsymbol{f}_{ext}$, $\boldsymbol{u}_n$ (previous step)

step 2: iteration $\nu+1$ (solve linear)

Step 2.1 element e

$\boldsymbol{d}\_ele \leftarrow \boldsymbol{u}_n$

Gauss point ξ_l

$\boldsymbol{C}^s / \boldsymbol{C}^s\_d.$

$\boldsymbol{B}\{e, \xi_l\}$, $\boldsymbol{d}\_ele$ $\longrightarrow \boldsymbol{F}(\xi_l) \longrightarrow$ $\boxed{SVK\_Material\ Model}$

$\downarrow$

$\boldsymbol{D}(\xi_l), \boldsymbol{T}(\xi_l), \boldsymbol{\Sigma}(\xi_l)$

$\downarrow$

$\boldsymbol{K}\_ele$, $\boldsymbol{f}\_int\_ele$

end

Step 2.2 Assembly : $\boldsymbol{K}^{\nu+1}$, $\boldsymbol{f}\_int^{\nu+1} \Rightarrow \boldsymbol{f}^{\nu+1} = \boldsymbol{f}_{ext} - \boldsymbol{f}_{int}^{\nu+1}$

2.3. Apply B.C. : $\boldsymbol{K}\_reduced^{\nu+1}$, $\boldsymbol{f}\_reduced^{\nu+1}$

2.4. Solve Linear : $d\boldsymbol{u}^{\nu+1}\_reduced = \boldsymbol{K}\_reduced^{\nu+1} \backslash \boldsymbol{f}\_reduced^{\nu+1}$

$d\boldsymbol{u}^{\nu+1} \leftarrow$

2.5 check convergence : $\| d\boldsymbol{u}^{\nu+1} \|$ vs. tol

$\| d\boldsymbol{u} \| > tol$ → step 2

$\| d\boldsymbol{u} \| < tol$ → Step 1, $U_{n+1} = U_n + du$

3 Numerical Solutions

For mesh options of 2x20, 4x40, 8x80, we obtained the numerical results by FI, RI, SRI respectively. All the numerical results were got with settings, load steps = 5 and tolerance for convergence = 10^{-4}.

3.1 Load(P) - deflection(u_y) response at the centroid of the load end

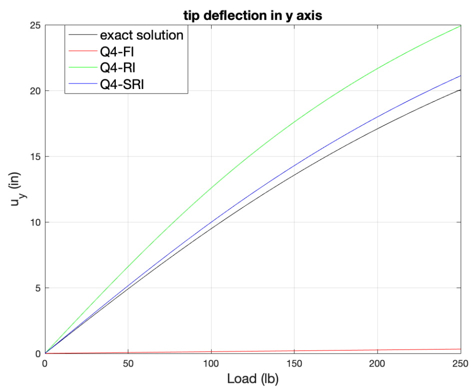

(a) Mesh = 2x20

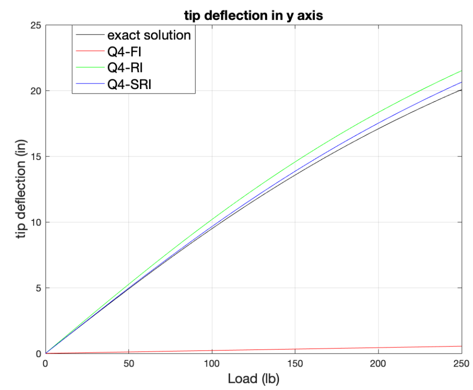

(b) Mesh = 4x40

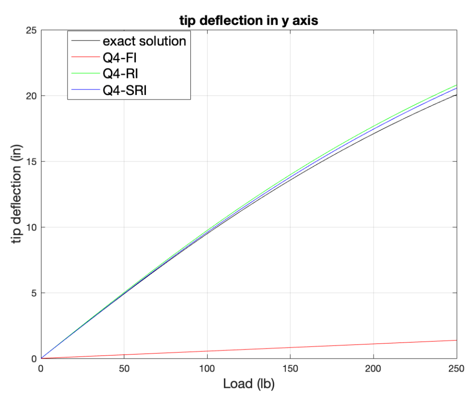

(c) Mesh = 8x80

Figure 2: Numerical results of tip deflection with different mesh refinements

From the figures above, we can observe that the solutions by FI 'locks' in all the three mesh refinements. However, the results by RI and SRI are very close to the reference solution in (c) mesh = 8x80. And the results by SRI have less error than the results by RI.

3.2 Displacement solution u_y along $y = 0$ at $P = 250lb$

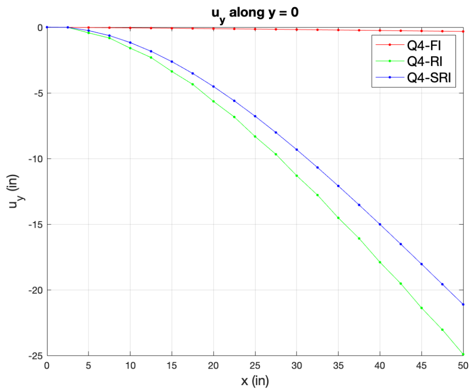

(a) Mesh = 2x20

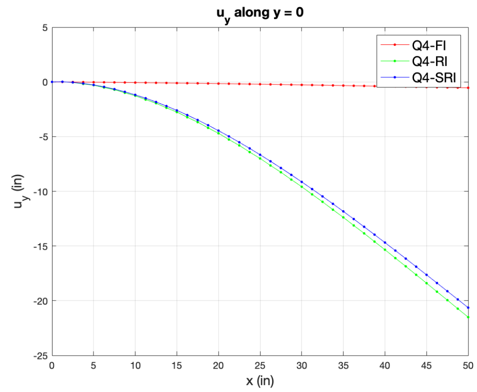

(b) Mesh = 4x40

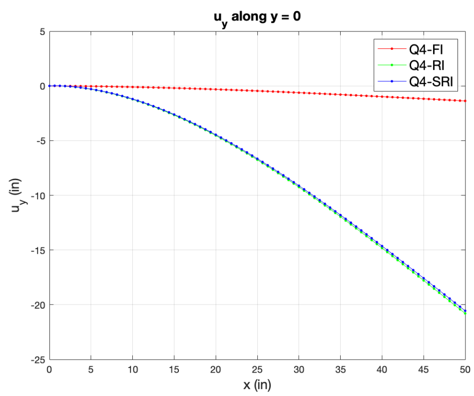

(c) Mesh = 8x80

Figure 3: Numerical results of u_y along $y = 0$ with different mesh refinements

From the figure above, we can see the results by RI approaches SRI as we refined the mesh, while the results by FI still locks. Then we can implement that we should use refined mesh when using RI in order to get accurate results.

3.3 Stress solutions along $x = L/2$ at $P = 250lb$.

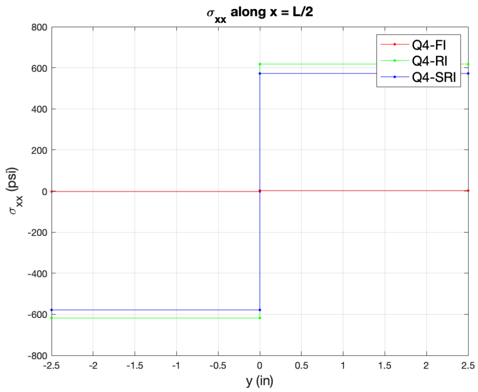

(a) Mesh = 2x20

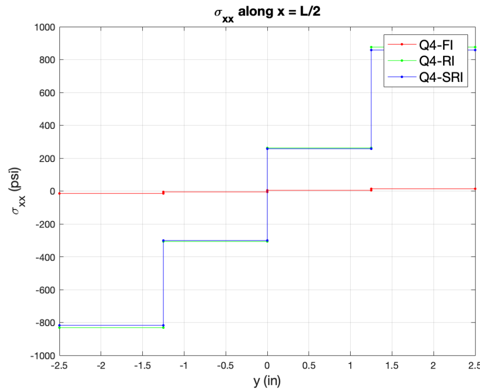

(b) Mesh = 4x40

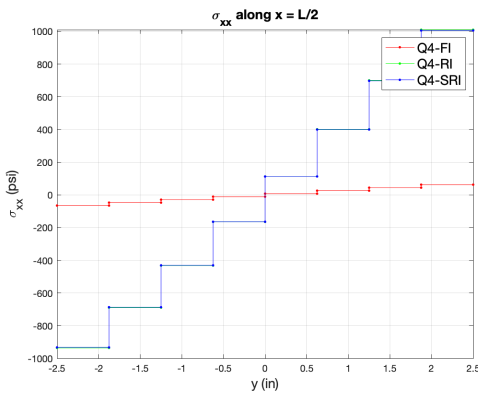

(c) Mesh = 8x80

Figure 4: Numerical results of σ_{xx} along $x = L/2$ at $P = 250lb$ with different mesh refinements

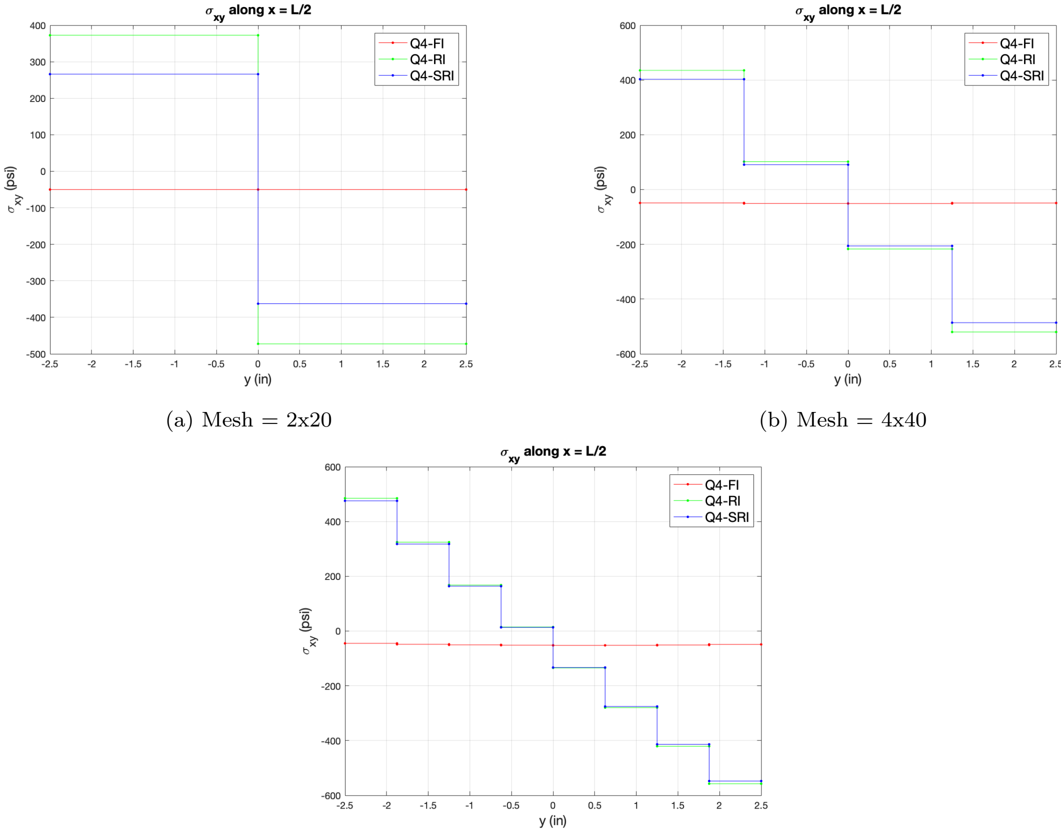

(a) Mesh = 2x20 (b) Mesh = 4x40

(c) Mesh = 8x80

Figure 5: Numerical results of σ_{xy} along $x = L/2$ at $P = 250lb$ with different mesh refinements

From the results of σ_{xx} and σ_{xy} along $x = L/2$ at $P = 250lb$, we can also observe the 'locking' of FI. And the results of SRI and RI are getting more and more identical to each other when we refined the mesh. And it also meets the mechanical expectation that the stresses increase from $y = 0$ to the upper and lower surfaces.

4 Discussion

4.1 Analysis of the Integration Methods

The figure below shows the shape of the beam after deformation with different integration methods by 2x20 meshing.

From the numerical results in Section-3, we can observed incompressible locking when using full integration. In Fig.6-a below, it is more obvious that the beam becomes so stiff that it 'locks' even under large load. Then we introduce RI to resolve locking, which only uses one point integration per element. In Fig.6-b, we can see the beam no longer locks. However, there occurs another problem, the Hourglass modes, shown in Fig.6-d: an enlarged part of Fig.6-b. Here we can find the elements have 'zigzags' on element boundary, which are the so-called 'Hourglass modes'. Finally, we used SRI to stabilize the hourglass instability. As we can observe in Fig.6-c, the mesh in the beam becomes smooth and the hourglass modes disappear.

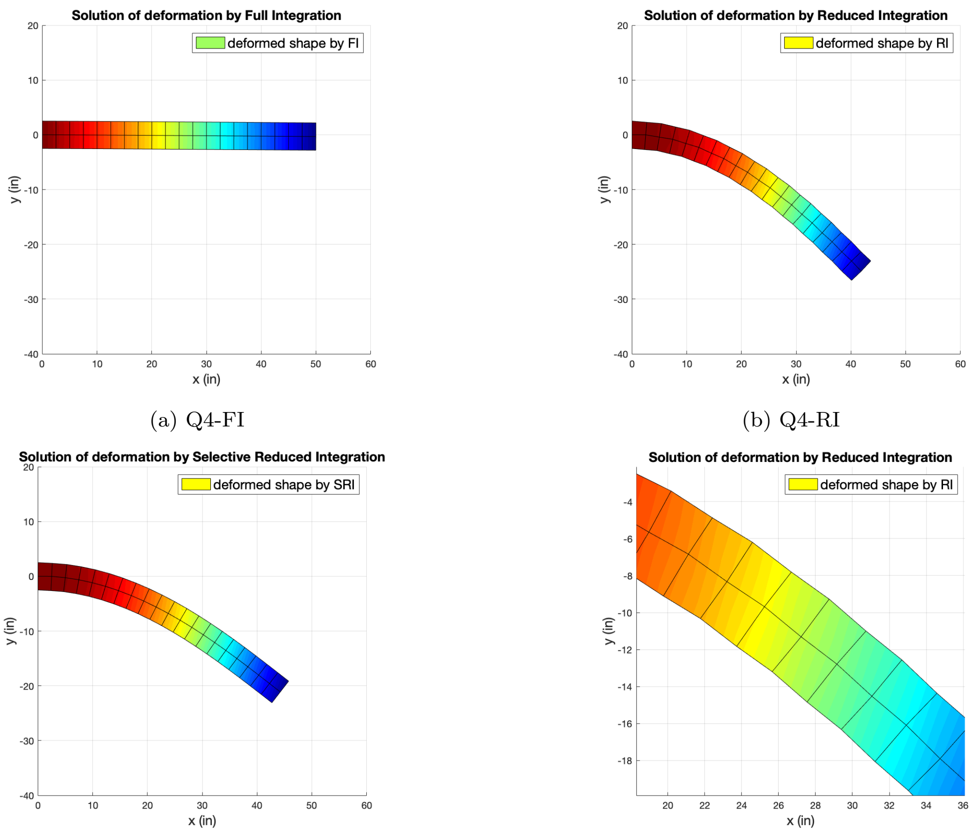

(a) Q4-FI

(b) Q4-RI

(c) Q4-SRI

(d) Q4-RI(enlarged)

Figure 6: Deformed shapes of beam when mesh = 2x20

4.2 The Effect of Mesh Refinements on the Accuracy of Displacements and Stresses

To study the effect of mesh refinement on accuracy, we can estimate the error of displacement by FI, RI and SRI, with 2x20, 4x40 and 8x80 meshing. In Fig.7, the x axis is log(number of elements in x), representing mesh refinements. This means we have finer mesh when x is large. And the y axis is the absolute value of error for u_y at the tip centroid when $P = 250lb$. For all the three integration methods, error decreased as we refine the mesh. However, the error for FI does not converge to zero while the other two converge.

Regarding the results of stresses, recalling Fig.4 and 5, we find the results of RI get closer to the results of SRI, which is set as the reference, as we refine the mesh. However, the results of FI could hardly be improved by mesh refinement.

Then we can conclude the locking effect in FI cannot be resolved by mesh refinement. But the results accuracy of RI and SRI (especially RI) can be greatly improved with finer mesh. And the results by SRI are more accurate than the results by RI because it uses more integration points to increase accuracy and also avoid hourglass instability.

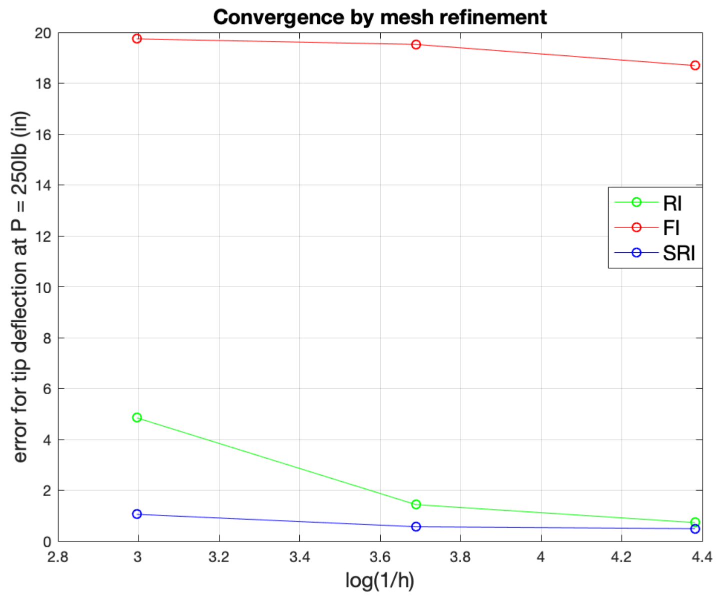

Figure 7: Error of u_y at the tip centroid vs. mesh refinement